1) S. C. West, et. al., “Alignment and use of the optical test for the 8.4 m off-axis primary mirrors of the Giant Magellan Telescope”, Proc SPIE, 7739, 7739ON (2010).

Now that the SFS CoC point is positioned relative the measurement hologram, Figure 9 illustrates how the Point Source microscope (PSM) is used to align the SFS to the CoC ball in the Cradle. The PSM (Optical Perspectives Group, Tucson AZ) is an autocollimator and source with a detector for centroiding the return beam. A 20x microscope objective diverger is attached to the output. The PSM is mounted to a remotely controlled positioner, and is aligned to center the return beam that reflects from the surface of the CoC ball. When the CoC ball is removed, the PSM fills the SFS, and the SFS positioners are adjusted to align the SFS position and orientation to the CoC ball center using the detector of the PSM. The SFS radius of curvature has been previously measured by using a laser tracker to measure the distance between the CoC ball and an SMR contacting the SFS surface in several locations.

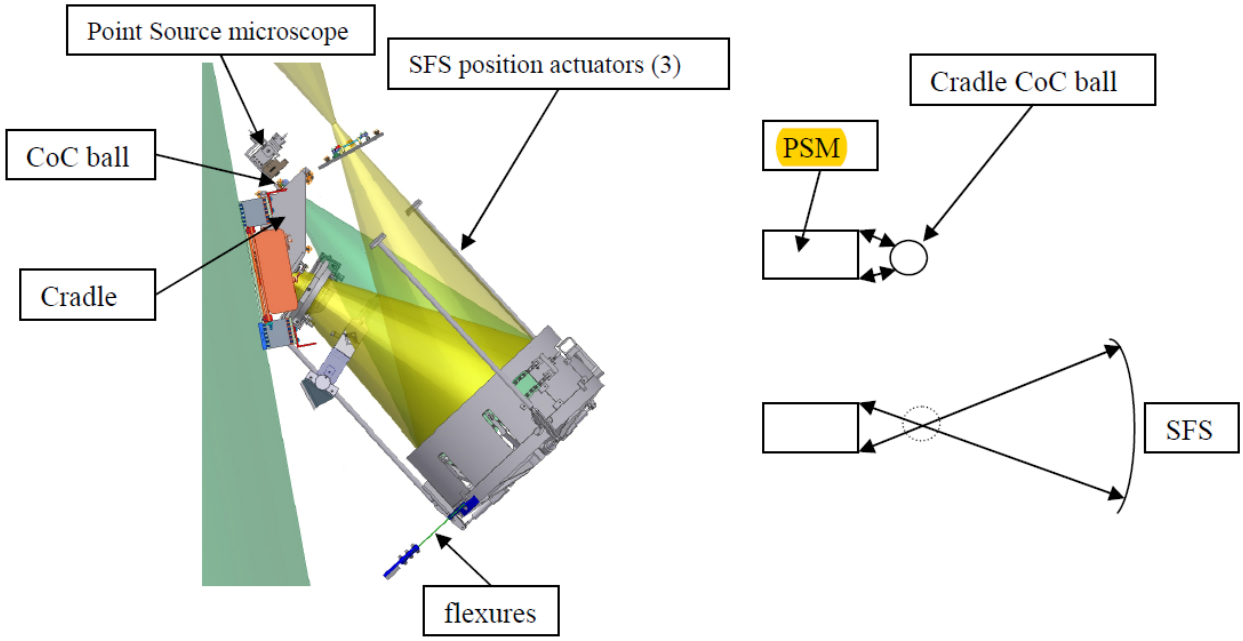

Figure 9: Use of the Point Source microscope (PSM) to adjust the position and orientation of the SFS is shown in a side view of Sam (left). The PSM is aligned to the SFS CoC ball in the Cradle (upper right). The ball is removed, and the SFS position actuators are adjusted to bring the SFS radius of curvature point to the ball center (lower right).

4) J. H. Burge, et. al., “Development of surface metrology for the Giant Magellan Telescope primary mirror”, 7018, 701814 (2008).

The components of SAM are mounted in a steel frame attached to the third platform of the test tower, Fig. 6. Critical dimensions are maintained by a small invar frame (the cradle) that supports the measurement hologram and a ball at the center of curvature of M2 (the M2 CoC ball), and by three invar metering rods that constrain M2 relative to the cradle in piston, tip and tilt. The cradle is mounted kinematically in the steel frame, with no adjustments. The M2 ball and the hologram are separated by only 440 mm, so the cradle can be relatively small.

Figure 6. The invar cradle is used to provide the reference for the most critical dimensions in the optical test. The position of M2 is adjusted so that its center of curvature coincides with the M2 reference ball, which is attached to the cradle. The position of this reference ball, with respect to the CGH is controlled to < 10 μm over the distance of 44 cm.

5) H. M. Martin, et. al., “Fabrication and testing of the first 8.4 m off-axis segment for the Giant Magellan Telescope”, Proc. SPIE 7739, 77390A (2010)

Alignment tolerances for this optical test are challenging, in part because of the lack of symmetry. We developed techniques based on CGHs, laser trackers and a point-source microscope (PSM) to align the interferometer and first two elements of the null corrector to accuracy on the order of 10 μm, and the full system including the GMT segment to the order of 100 μm.

6) M. Tuell, et. al., “Final acceptance testing of the LSST monolithic primary/tertiary mirror”, Proc. SPIE, 9151, 91510W (2014)

Both surfaces must have their optical axis within 1 mm of the mechanical axis of the blank, and must be within 1 mm of each other. Axis decentration is equivalent to coma in the surface, so we call these "coma tests". A fixture was prealigned in the lab such that a crosshair is within 0.002" (50 µm) of the mechanical ID of the mirror, which we define as the mechanical axis of the blank. Rotating the fixture while on the mirror verifies how well centered the crosshair is, and it does appear to be within 25-50 µm of the true mechanical axis. A removable camera is placed above the crosshair in a kinematic mount, for which we know the mirror center pixel to within 50 µm. The reticle is used for the traditional rotation test and the camera is for the projected spot test, as described in the next sections. A photograph of the center fixture on the air bearing, with a point source microscope (PSM) aligned to the bearing axis, is shown in Figure 8. Both methods have approximate uncertainties of ± 0.25 mm, so we need to get the two mirrors aligned to within about 0.5 mm of each other to guarantee that they are truly within the 1 mm tolerance.

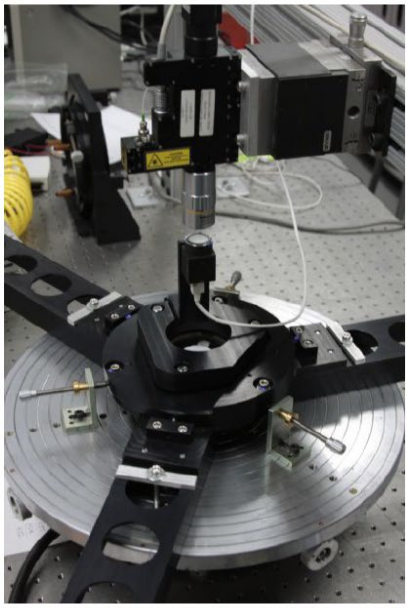

Figure 8 - Coma test fixture with both crosshair and camera (in a kinematic mount) on a rotary air bearing with a point-source microscope to define the axis of rotation.

8) M. Johns, et. al., “Progress on the GMT”, Proc. SPIE, 7018, 70180C (2008)

In-process testing of the GMT segments uses a phase-shifting interferometer capable of imaging the full surface of GMT1 in a single frame. The test configuration is shown schematically in Figure 5. The segments are tested face-up in the tower. A 3.75 m diameter spherical mirror at the top folds the beam and allows the test to fit within the maximum height of the polishing lab. This fold mirror also removes most of the astigmatism introduced by viewing the off-axis segment face-on. The interferometer assembly (SAM) contains a second fold sphere to provide additional correction and a computer generated hologram (CGH) to correct residual wavefront errors. The removable Alignment CGH and Point Source Microscope (PSM) provide the means to align the internal components of SAM and align SAM with respect to the rest of the test optics.

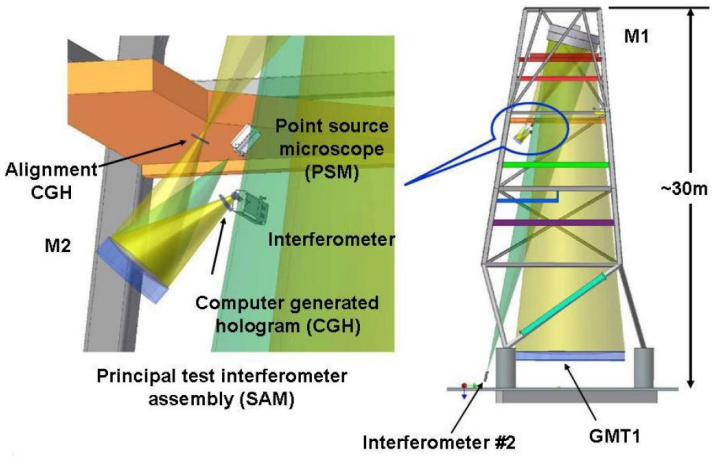

Figure 5. Principal Test configuration.

9) R. Allen, et. al., “Scanning pentaprism test for the GMT 8.4 m off-axis segments” Proc SPIE, 7739, 773911 (2010)

Figure 12 shows the Apogee Instruments Alta U16000 CCD camera that was selected for use in the pentaprism test. The Kodak KAI-16000M chip in this camera has an active area of 36 x 24 mm, and the pixels are 7.4 x 7.4 microns in size. The figure shows a point source microscope (PSM) being used to determine the position of the camera chip with respect to four tracker balls on its mounting plate.

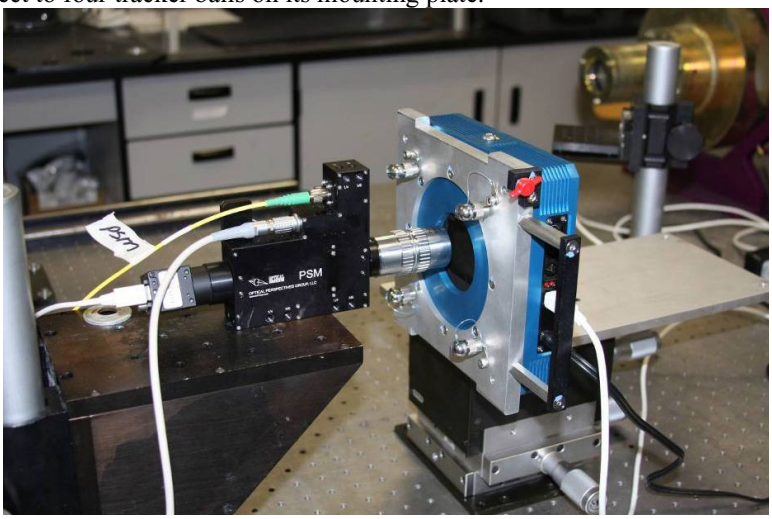

Figure 12. The Alta U-16000M camera used in the pentaprism test. The point source microscope (PSM) on the left is being used to measure the position of the camera chip with respect to the four tracker balls on its mount. The laser tracker itself is out of view to the left.

10) S. Sankar and J. Livas, "Testing and characterization of a prototype telescope for the evolved Laser Interferometer Space Antenna (eLISA)", Proc. SPIE, 9904, 99045A (2016)

The alignment of the system proceeds as follows. Firstly, a point-source-microscope is used to illuminate M1 from near the primary's focus point. M1 is a parabola, so illumination from the focus produces a large, collimated beam. This beam is then retro-reflected off a large autocollimating flat, back into the point-source-microscope. Minimization of the spot diameter and asymmetry as seen from the point-source-microscope camera ensures the autocollimating flat is aligned to the primary. The alignment of the autocollimating flat to the primary mirror is checked by theodolite and compared to the optical model to ensure consistency.

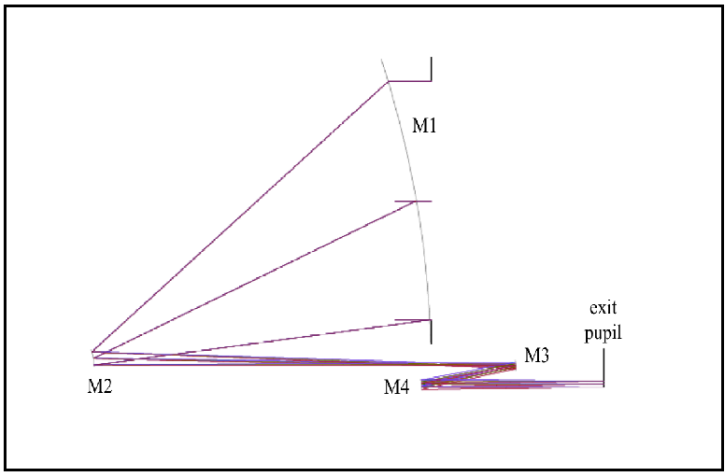

Figure 1. A simple schematic of the baseline layout for the off-axis reference design

27) C. Peng, et. al, "Calibration method of shear amount based on the optical layout of point source microscope for lateral shearing interferometric wavefront sensor," *Optical Engineering* 59(9), 094106 (26 September 2020). (Shanghai Institute of Optics and Fine Mechanics, Shanghai, China)

First, an alignment step is required to ensure that the optical axis is perpendicular to the sensitivity plane of the sensor. In this step, the objective lens is removed and the PSM is in the autocollimator mode. (It is worth noting that the PSM works as an electronic autocollimator when the objective lens is removed because the microscope is based on infinite conjugate optics.[28]) A collimated beam exits the PSM and is reflected by the sensitivity plane of the sensor. Then the reflected beams are focused by the lens before the PSM camera, depicted in green dashed lines in Fig. 12(a). Adjust the tilt of the wavefront sensor so that the reflected image is focused on the center of the PSM camera and is centrosymmetric to the crosshairs of the PSM camera. By now, the precalibration alignment step is finished and the sensitivity plane of the sensor is considered as being perpendicular to the optical axis.

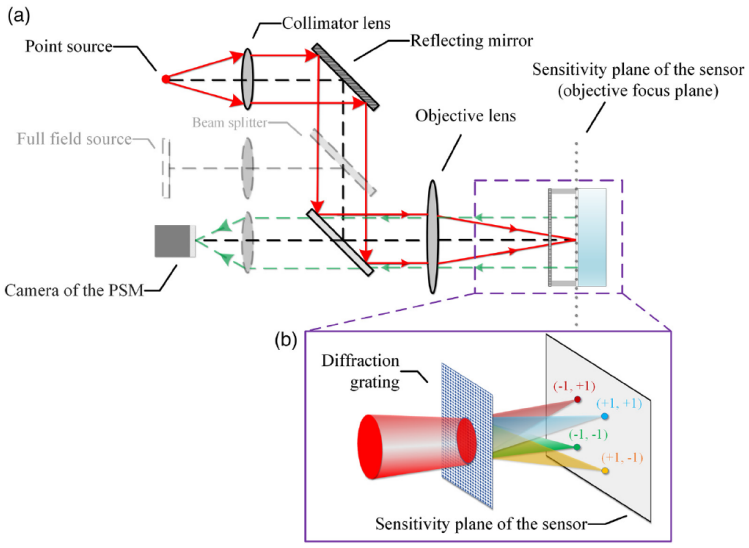

Fig. 12 The principle of the calibration method based on the optical layout of PSM. (a) The overall optical layout. (b) Detailed illustration when the convergent beam enters the wavefront sensor.

34) A. Lowman, "Measurement of large on-axis and off-axis mirrors using software configurable optical test system (SCOTS)", Proc. SPIE 10706, Advances in Optical and Mechanical Technologies for Telescopes and Instrumentation III, 107061E (10 July 2018) (College of Optical Sciences, University of Arizona)

Figure 10 shows photographs of the GMT SCOTS hardware. The hardware is mounted on a tray (left) that slides in front of the interferometric test. The camera is located in a well, which made it impractical to mount SMRs around its barrel as was done for DKIST and the 6.5 m project since the laser tracker could not view them. Instead, the SMRs are mounted at the top of the camera subassembly (right). The picture shows a PSM mounted to a CMM (which was essentially used as a translation stage with encoder), with the PSM focused at the center of an SMR. The camera is mounted to manual translation stages above a rotation stage, with the translation stages used to align the pinhole to the rotation axis. The rotation stage allows measurements to be taken at different camera angles, to average errors introduced by the lenses.

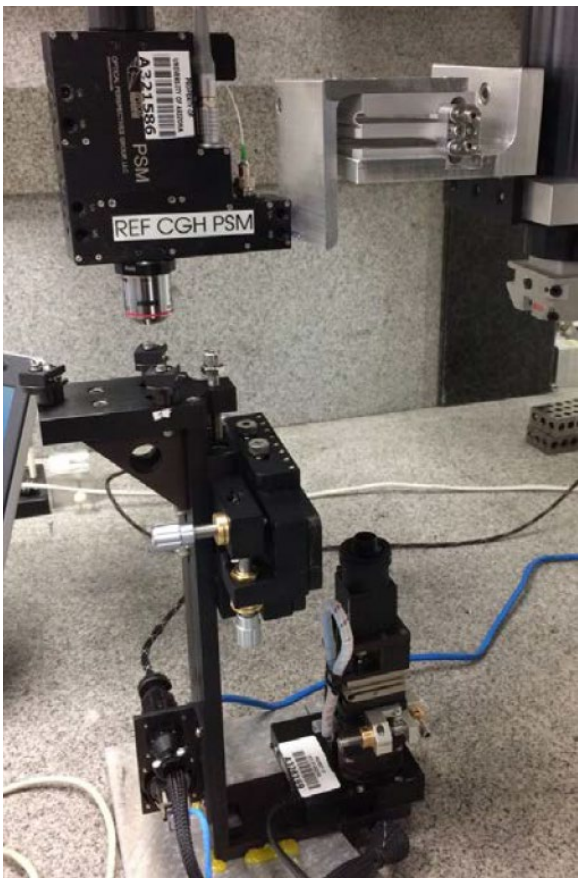

Figure 10. Close up of camera subassembly during calibration. PSM is focused on an SMR.

35) M. Tuell, et, al., “Fabrication of the LSST monolithic primary-tertiary mirror”, Proc SPIE, 8450, 84504Q (2012) (Steward Observatory, University of Arizona)

The alignment of the small mirror on the tripod will be accomplished with the use of a laser tracker and spherically mounted retroreflector (SMR), rotary air bearing and a point source microscope[9] (PSM). This procedure should be sufficient without the use of a rotary table, but the ability to rotate the system while looking at the reflection with the PSM gives an additional level of confidence. Some parts of this system are shown in Figure 8.

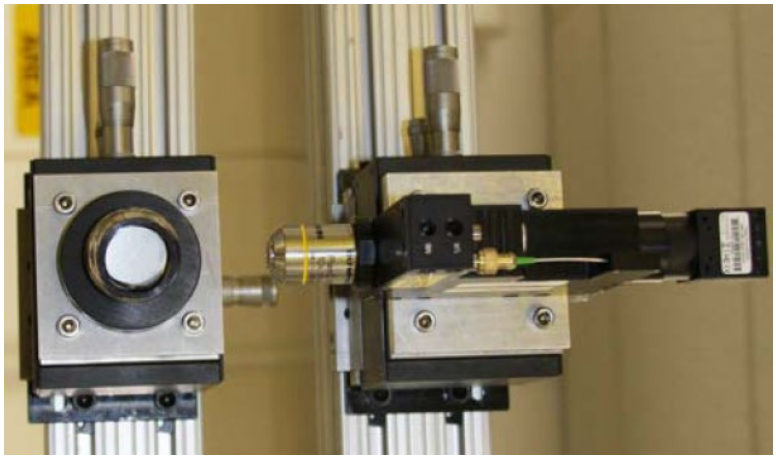

Fig. 8 PSM/tracker

37) Kaiyuan Zhang, et. al., “High Numerical Aperture Multimode Fibers for Prime Focus Use”, Proc. SPIE, 9912, 99125J (2016)

For astronomical use, consistency of the near field distribution at the fiber output is very important, as any change causes errors in the sky subtraction, and in the inferred spectral profile and velocity of the target. A desirable property of fibers is that the azimuthal distribution of light should be completely scrambled, in both near- and far-field for long length fibers [3]. To test for this effect, we constructed an experimental setup as shown in Figure 13. The fiber is mounted in the same way as in FRD measurement setup. The point source microscope (PSM) is used as the input beam source with a 10X microscopic lens of NA 0.25 to inject into the fiber, and the input fiber to the PSM is single mode fiber with core of 5.3μm. Since the PSM is built with an input surface inspection tool, it is much easier for monitoring the relative input beam position on the fiber as shown in Figure 13. The other end of the fiber surface is re-imaged by an objective lens of NA 0.3 on a second CCD camera, and by calculating the image centroid; the near field performance can be verified.

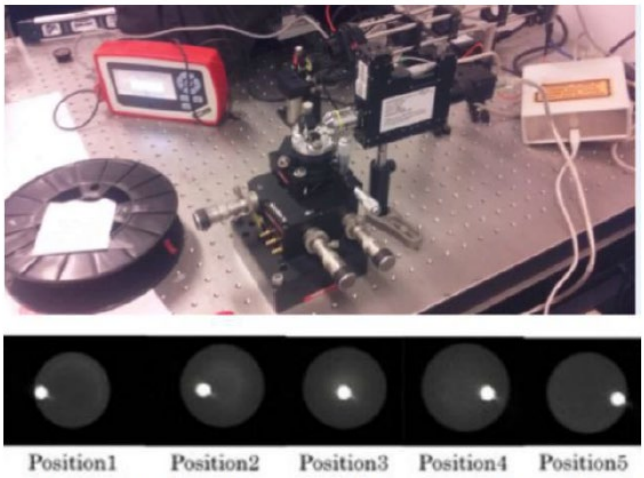

Figure 13: Input beam position captured by PSM

42) H. Durazo, et. al., “Design and implementation of a new time-delayed source and alignment considerations for a tangent ogive interferometer”, Proc SPIE, 7302, 730215 (2009)

The initial step to align the interferometers is to center the base that supports the tangent ogive with the axis defined by the center of rotation of the rotary stage. This is accomplished by focusing a Point Source Microscope[3] (PSM) at the center of curvature of a precision ball-bar. As the rotary stage spins, the x and y stages are adjusted until the location of the center of the ball as observed by the PSM does not move. Next, the tip and tilt on the rotary stage are adjusted to level the base. This is done mechanically by minimizing the total indicated runout (TIR) of the base plate as the stage is rotated. Once the rotary stage is centered and leveled, the outer ball of the ball-bar is used to define the location of the center of curvature of the tangent ogive. Figure 6 below shows the rotary stage with the ball-bar.

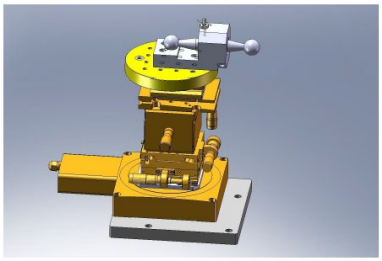

Figure 6. Rotary stage with ball-bar.

43) R. Boye, et. al., “Design of Wearable Binoculars with On-Demand Zoom”, Proc SPIE, 8841, 88410H (2013)

The final mirror to be aligned was the freeform element. An initial alignment sensitivity analysis indicated that the alignment tolerances for this element were fairly large, e.g. 50 μm or more for lateral alignment, but it was decided to do an active alignment of this element to insure the best alignment could be achieved repeatably. A collimator and point source microscope were setup to actively measure the output of the design while the final mirror was aligned. The point source microscope (PSM) was used with its objective removed to test the collimated output of the full prototype. The operator could manipulate the mirror while minimizing the focused spot produced by the optical assembly, see Figure 6. Care was taken to initially align the collimator and point source microscope (PSM), but the alignment of the final mirror was found to be straightforward and repeatable.

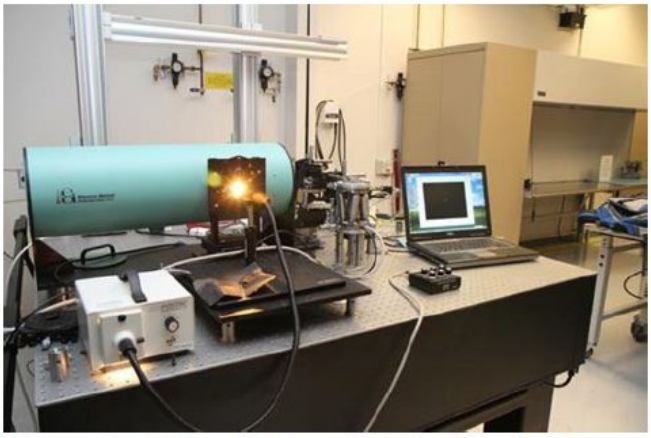

Figure 6. Active alignment station for freeform mirror placement.

44) P. Su, et. al, “Aspheric and freeform surfaces metrology with software configurable optical test system: a computerized reverse Hartmann test”, Opt. Eng., 53(3), 031305 (2014)

Figure 4 shows how the camera pinhole can be calibrated into the test coordinate system. A point source microscope (PSM) mounted on a CMM is used to optically relate the camera pinhole position to three tracker balls attached to the camera. In this way, anytime the locations of the three balls are measured with a laser tracker, the pinhole position can be calculated based on the calibration data.

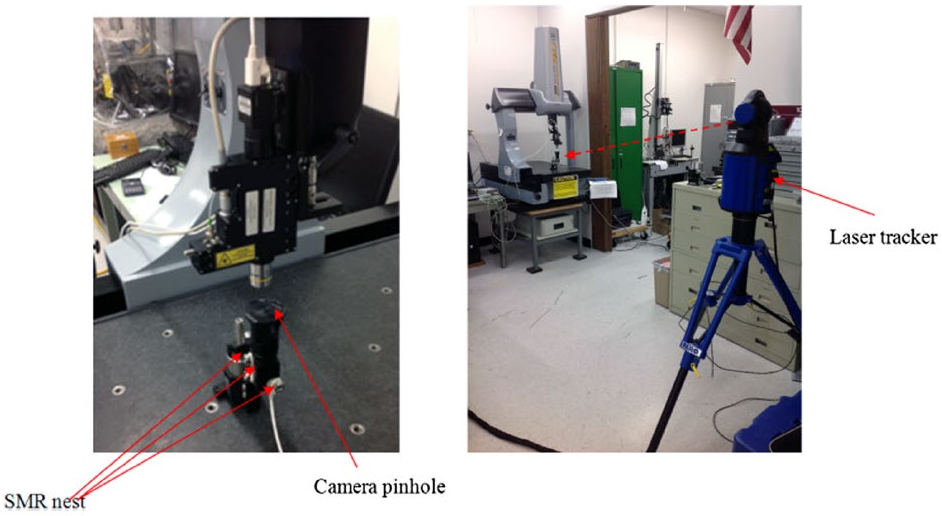

Fig. 4 Camera pinhole location calibration with a laser tracker (SMR: spherical mounted retroreflector).

45) L. Coyle, et. al., “Design and analysis of an alignment procedure using computer-generated holograms”, Opt. Eng., 52(8), 084104 (2013).

The residual alignment error was measured with an independent optical test. In the region outside the FZPs, two extra patterns on each CGH act like two sets of spherical mirrors
with a sphere on CGHA having a common “center of curvature” with a sphere on CGHB. When a point source is placed at the center of curvature for one set of mirrors, the displacement between the reflected spots shows the CGH misalignment, as in Fig. 15. Two sets of mirrors are needed to calculate the tilt and centration misalignments of CGHB to CGHA in both the x- and y-directions.

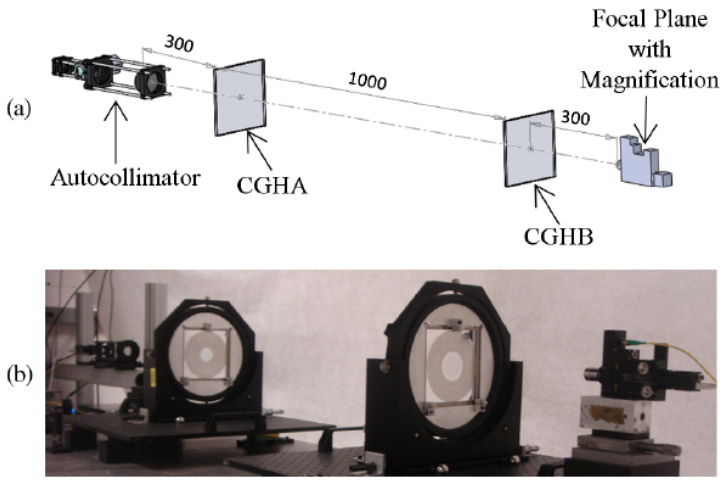

Fig. 14 (a) The optical system consists of two CGHs spaced 1 m apart with the autocollimator and focal plane on either end (distances in millimeters). (b) The experimental setup is pictured.

46) L. Coyle, et. al., “Low uncertainty alignment procedure using computer generated holograms”, 8131, 81310B (2011)

Figure 7 demonstrates this process for centration. We align a video microscope to the far spot and set its centroid position as the reference point. We then eliminate the far spot by stopping down the iris on the autocollimator so the outer annulus of CGH1 is no longer illuminated. We insert CGH2, and see only the re-imaged near spot. Since the spot is displaced from the reference point, we know CGH2 is decentered.

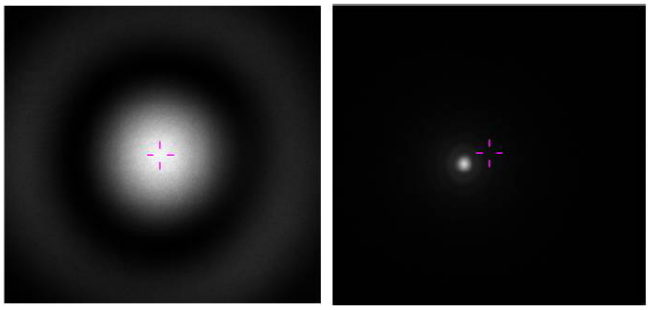

Figure 7. In the PSM Align software, we set the far spot as a reference point (left), stop down the autocollimator beam, then measure the displacement of the re-imaged near spot (right). The pictures have the same scale, but the far spot is larger than the near spot because the f/# of the beam is much slower.

47) J. Burge, et. al., “Optical alignment with computer generated holograms”, Proc SPIE 6676, 66760C (2007)

The alignment of the CGH itself can be performed by creating a pattern which uses Littrow diffraction to autoreflect the illumination wavefront as shown in Figure 4. For the case of a point source, the CGH is made to act as a spherical surface, with center of curvature at the source point. If the illumination is provided by an interferometer or a point source microscope (PSM), then it is possible to measure the reflection directly and move the CGH to the appropriate location.

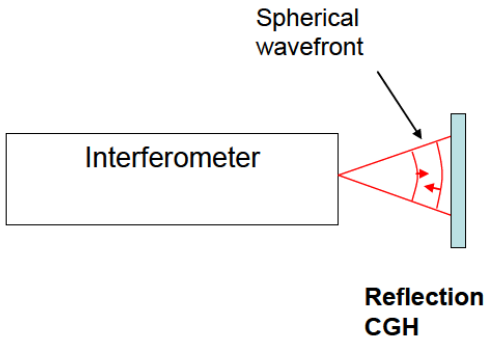

Figure 4. The autoreflection from the CGH is useful for aligning the CGH to the wavefront.